NASA CONTRACTOR REPORT

FATIGUE CRACK PROPAGATION IN 2024-T3 AND 7075-T6 ALUMINUM ALLOYS AT HIGH STRESSES

by Robert G. Dubensky

Prepared by
UNIVERSITY OF AKRON
Akron, Ohio 44304
for Langley Research Center

NATIONAL AERONAUTICS AND SPACE ADMINISTRATION • WASHINGTON, D. C. • MARCH 1971

1. Report No.	2. Government Accession No.	3. Recipient's Catalog No.
NASA CR-1732		

4. Title and Subtitle	5. Report Date
FATIGUE CRACK PROPAGATION IN 2024-T3 AND 7075-T6 ALUMINUM ALLOYS AT HIGH STRESSES	March 1971
	6. Performing Organization Code

7. Author(s)	8. Performing Organization Report No.
Robert G. Dubensky	
	10. Work Unit No.

9. Performing Organization Name and Address	11. Contract or Grant No.
University of Akron Akron, Ohio 44304	NGR-36-001-010
	13. Type of Report and Period Covered
12. Sponsoring Agency Name and Address	Contractor Report
National Aeronautics and Space Administration Washington, D. C. 20546	14. Sponsoring Agency Code

15. Supplementary Notes This report supplements material presented in "Effect of Stress Ratio on Fatigue-Crack Growth in 7075-T6 and 2024-T3 Aluminum-Alloy Specimens" by C. Michael Hudson, in NASA TN D-5390.

16. Abstract Stable fatigue-crack-growth rates were measured at high stresses in axial-load fatigue tests on 12-inch wide sheet specimens made of 7075-T6 and 2024-T3 aluminum alloys. These tests were made at stress ratios R (ratio of the minimum stress to the maximum stress) ranging from 0 to 0.7 and at maximum stress levels ranging from 55 to 72.5 ksi for the 7075-T6 alloy and 30 to 52.5 ksi for the 2024-T3 alloy. The elastic stress-intensity method was used to correlate the measured rates. In addition, a modified stress-intensity method was derived by combining Rice's cyclic stress-intensity method with the modified (for plasticity) stress-intensity method proposed by Irwin, Dugdale, and Newman. For a given R value, fatigue-crack-growth rates in 7075-T6 were nominally a single-valued function of the elastic stress-intensity range and of the modified stress-intensity ranges. At each R value, fatigue-crack-growth rates in 2024-T3 below a value of 1×10^{-4} in./cycle were nominally a single-valued function of the elastic stress-intensity range and of the modified stress-intensity ranges. However, fatigue-crack-growth rates in the 2024-T3 above approximately 1×10^{-4} in./cycle were ordered according to the maximum applied stress for all methods. Fatigue-crack-growth in 7075-T6 always became unstable and static fracture occurred as the fatigue-crack-growth rates approached 4×10^{-2} in./cycle, whereas stable fatigue-crack-growth rates up to 4×10^{-1} in./cycle were observed in 2024-T3. All curves of rate plotted against range of stress-intensity show the definite reflex curvature at the high R values in the 7075-T6 alloy and at most R values in the 2024-T3 alloy.

17. Key Words (Suggested by Author(s))	18. Distribution Statement
Fatigue-Crack Propagation 7075-T6 and 2024-T3 Aluminum Alloys Stress Intensity Plasticity	Unclassified - Unlimited

19. Security Classif. (of this report)	20. Security Classif. (of this page)	21. No. of Pages	22. Price*
Unclassified	Unclassified	30	$3.00

*For sale by the National Technical Information Service, Springfield, Virginia 22151

FATIGUE CRACK PROPAGATION IN 2024-T3 AND 7075-T6 ALUMINUM ALLOYS AT HIGH STRESSES

Robert G. Dubensky

at

UNIVERSITY OF AKRON

Akron, Ohio

ABSTRACT

Stable fatigue-crack-growth rates were measured at high stresses in axial-load fatigue tests on 12-inch wide sheet specimens made of 7075-T6 and 2024-T3 aluminum alloys. These tests were made at stress ratios R (ratio of the minimum stress to the maximum stress) ranging from 0 to 0.7 and at maximum stress levels ranging from 55 to 72.5 ksi for the 7075-T6 alloy and 30 to 52.5 ksi for the 2024-T3 alloy.

The elastic stress-intensity method was used to correlate the measured rates. In addition, a modified stress-intensity method was derived by combining Rice's cyclic stress intensity method with the modified (for plasticity) stress-intensity method proposed by Irwin, Dugdale, and Newman. For a given R value, fatigue-crack-growth rates in 7075-T6 were nominally a single-valued function of the elastic stress-intensity range and of the modified stress intensity ranges. At each R value, fatigue-crack-growth rates in 2024-T3 below a value of 1×10^{-4} in./cycle were nominally a single-valued

function of the elastic stress-intensity range and of the modified stress-intensity ranges. However, fatigue-crack-growth rates in the 2024-T3 above approximately 1×10^{-4} in./cycle were ordered according to the maximum applied stress for all methods.

Fatigue-crack-growth in 7075-T6 always became unstable and static fracture occurred as the fatigue-crack-growth rates approached 4×10^{-2} in./cycle, whereas stable fatigue-crack-growth rates up to 4×10^{-1} in./cycle were observed in 2024-T3. All curves of rate plotted against range of stress-intensity show the definite reflex curvature at the high R values in the 7075-T6 alloy and at most R values in the 2024-T3 alloy.

INTRODUCTION

Fatigue cracks may initiate early in the life of cyclically loaded structural components, ref. 1. Therefore, the useful life of these components is determined by the rate at which these fatigue cracks propagate. The rate of fatigue crack propagation was shown to be a function of the elastic stress intensity range, ΔK, and the stress ratio, R, for constant amplitude loading, ref. 2. To insure that the elastic stress-intensity analysis was applicable to the data generated in ref. 2, the ratio of the maximum applied stress to the yield stress was kept below 0.6. However, under actual service conditions (pressure vessels, for example) the ratio of the maximum applied stress to the yield stress can be much closer to 1. Accordingly, an investigation was conducted to study fatigue-crack-growth

rates produced by stresses approaching the material yield stress. Axial-load fatigue-crack-growth tests were conducted on sheet 7075-T6 and 2024-T3 aluminum-alloy specimens. The stress ratios used in these tests ranged from 0 to 0.7.

The data were analyzed by using stress-intensity analysis methods. These methods included the elastic stress-intensity analysis, and a modified stress-intensity analysis derived by combining Rice's cyclic stress intensity method (ref. 3) with the modified (for plasticity) stress intensity methods proposed by Irwin (ref. 4), Dugdale (ref. 5), and Newman (ref. 6). A comparison was made between the capabilities of the different methods to correlate the data.

SYMBOLS

A	material constant
a	one-half of total length of a central symmetrical crack, inches
B	material constant
K	elastic stress-intensity factor, ksi-in.$^{1/2}$
K_{max}	elastic stress-intensity factor corresponding to maximum cyclic stress, $\alpha S_{max} (\pi a)^{1/2}$, ksi-in.$^{1/2}$
K_{min}	elastic stress-intensity factor corresponding to minimum cyclic stress, $\alpha S_{min} (\pi a)^{1/2}$, ksi-in.$^{1/2}$
ΔK	range of elastic stress-intensity factor, $K_{max} - K_{min}$, ksi-in.$^{1/2}$

$\Delta K_{(D)}$	range of stress-intensity factor including the correction for plasticity proposed by Dugdale, ksi-in.$^{1/2}$
$\Delta K_{(Irwin)}$	range of stress-intensity factor including the correction for plasticity proposed by Irwin, ksi-in.$^{1/2}$
$\Delta K_{(N)}$	range of stress-intensity factor including the correction for plasticity proposed by Newman, ksi-in.$^{1/2}$
N	number of cycles
P_a	amplitude of load applied in a cycle, kips
P_m	mean load applied in a cycle, kips
P_{max}	maximum load applied in a cycle, $P_m + P_a$, kips
P_{min}	minimum load applied in a cycle, $P_m - P_a$, kips
R	ratio of minimum stress to maximum stress
S	applied stress, ksi
S_a	alternating stress, P_a/wt, ksi
S_m	mean stress, P_m/wt, ksi
S_{max}	maximum gross stress, P_{max}/wt, ksi
S_{min}	minimum gross stress, P_{min}/wt, ksi
ΔS	range of applied stress, ksi
t	specimen thickness, inches
w	specimen width, inches
α	correction for finite width of panel, $(\sec \frac{\pi a}{w})^{1/2}$
ρ	actual plastic zone size, inches
$\rho_{(D)}$	plastic zone size proposed by the Dugdale model, inches
$\rho_{(Irwin)}$	plastic zone size proposed by the Irwin model, inches
$\rho_{(N)}$	plastic zone size proposed the Newman model, inches

σ_y material yield stress, ksi

SPECIMENS, TESTS, AND PROCEDURES

Specimens

The 7075-T6 and 2024-T3 aluminum-alloy sheet material tested was taken from the special stock retained for fatigue testing at the NASA Langley Research Center. Reference 7 gives the fatigue properties of this material. Table 1 lists the tensile properties obtained by using standard ASTM specimens and testing methods.

Fatigue crack growth experiments were conducted on sheet specimens 12 inches wide, 35 inches long and with a nominal thickness of 0.090 inch, figure 1. A crack starter notch 0.10 inch long by 0.01 inch wide was cut into the center of each specimen by an electrical discharge process. Since only very localized heating occurs in this process, virtually all of the material through which the fatigue crack propagates is unchanged by the cutting process. The longitudinal axis of all specimens was parallel to the rolling direction of the sheets.

A reference grid with lines spaced 0.050 inches apart was photographically printed on the surface of the specimen to measure crack growth. Previous metallographic examination and tensile tests of specimens with this grid indicated that it had no damaging effect on the material.

Testing Machine

The fatigue testing machine used was a combination subresonant

and hydraulic machine with a capacity of 132,000 pounds, ref. 8. All tests in this investigation were conducted using the hydraulic mode of operation with operating frequencies ranging from 4 to 25 cpm. Loads were continuously monitored on this machine by measuring the output of a strain-gage bridge on a dynamometer in series with the specimen. The maximum loading error was ±1 percent of the applied load.

Test Procedure

Axial-load fatigue crack propagation tests were conducted at stress ratios of 0, 0.33, 0.5, and 0.7 for the 7075-T6 and the 2024-T3 aluminum alloys. Tests were conducted at a number of maximum stress levels for a given stress ratio. These values ranged from 55 ksi to 72.5 ksi for 7075-T6, and from 30 ksi to 52.5 ksi for the 2024-T3 alloy. Both alternating and mean loads were kept constant throughout each test. Duplicate tests were conducted at selected stress levels to establish the repeatability of results in each material. All other results are based on the test of a single specimen.

In all of the tests, the specimens were clamped between guide plates to prevent buckling and out-of-plane vibrations during testing. A lightly oiled paper liner was inserted between the surfaces of the specimen and the guides. None of the oil was observed to enter the crack during testing; thus, the oil was not expected to affect the crack growth. A cutout one-inch wide across one of the guide plates permitted the crack tip to be observed.

Fatigue-crack-growth data were obtained using a 70 mm close-up camera which was activated by an electronic system. Initially photographs were taken after every 100 cycles of applied load, and this interval was continually decreased until photographs were taken as often as every cycle when the crack growth rates were high near the end of each test. This system photographed the cracked section of the specimen at the maximum applied load to obtain maximum crack definition, and superimposed an image of the machine's cycle counter. Thus, each frame of film showed the crack in the specimen, the reference grid, and the number of applied load cycles. Accurate crack-length-against-cycles curves were obtained from the data on these films.

All tests were conducted under controlled laboratory conditions with a nominal temperature of 74° F and a nominal relative humidity of 75 percent.

RESULTS AND DISCUSSION

Fatigue-Crack-Growth Data

Data resulting from the fatigue-crack-growth tests conducted on 7075-T6 and 2024-T3 specimens are presented in Tables 2 and 3. These tables show the average number of cycles required to produce cracks of equal length, a, on both sides of the specimens. The longest crack length shown in each a column was the length measured one or two cycles before final specimen failure occurred. Fatigue-crack-growth rates, da/dN, presented in this paper were determined by graphically

measuring the slopes of the crack growth curves defined in Table 2 and Table 3.

Elastic Stress Intensity Analysis of Data

Fatigue-crack-growth rates from this investigation (noncircular symbols), and from the investigation reported in reference 2 (circular symbols), are plotted against the elastic stress-intensity range, ΔK, in figure 2. (A brief discussion of the elastic stress-intensity analysis is given in the Appendix). For a given positive stress ratio, the crack growth rates in 7075-T6 were nominally a single-valued function of ΔK for all stress levels. Similarly, crack growth rates in 2024-T3 below approximately 1×10^{-4} in./cycle were nominally a single-valued function of ΔK. However, crack growth rates in 2024-T3 above 1×10^{-4} in./cycle were not. These higher rates were ordered according to the stress level, i.e., the higher the value of S_{max} in the test, the higher the rate of crack growth for a given value of ΔK.

Two additional observations can be made from figure 2. First, all fatigue-crack-growth rates in 7075-T6 were below 4×10^{-2} in./cycle, indicating that fatigue-crack-growth rates became unstable and static fracture occurred as they approached this value. However, stable fatigue-crack-growth rates up to 4×10^{-1} in./cycle were observed in 2024-T3. Second, figure 2 shows that a pronounced reflex curvature occurs at the high R values in the 7075-T6 alloy and at most R values in the 2024-T3 alloy (as predicted in reference 2).

Modified Stress Intensity Analysis of Data

Fatigue-crack-growth data from this investigation and from the investigation reported in reference 2, were also analyzed using a modified stress-intensity analysis derived (see the Appendix) by combining Rice's cyclic stress-intensity method with the modified (for plasticity) stress-intensity method proposed by Irwin (ref. 4), Dugdale (ref. 5), and Newman (ref. 6). For a given positive stress ratio, crack growth rates in 7075-T6 were nominally single-value functions of the modified stress-intensity range regardless of whether the Irwin, Dugdale, or Newman plasticity correction was used, figure 3.

As with the elastic stress-intensity analysis, crack growth rates in 2024-T3 below approximately 1×10^{-4} in./cycle were nominally a single-valued function of ΔK regardless of whether the Irwin, Dugdale, or Newman plasticity correction was used. However, crack growth rates in 2024-T3 above 1×10^{-4} in./cycle were not. Figure 4 shows these higher rates ordered according to the stress level, i.e., the higher the value of S_{max} in the test, the higher the rate of crack growth for a given value of ΔK.

Figure 2(a), and figures 3(a), 3(b), and 3(c) indicate that for 7075-T6 the elastic and modified stress-intensity analysis methods correlate the data equally well. Likewise figure 2(b), and figures 4(a), 4(b), and 4(c) indicate that for 2024-T3 the elastic and modified stress-intensity analysis methods correlate the data equally well at

rates below 1×10^{-4} in./cycle. However, neither the elastic nor modified stress-intensity method correlate the data at rates above 1×10^{-4} in./cycle. Results in reference 6 indicate that the modified stress-intensity method is able to correlate fracture toughness data on relatively tough materials with varying degrees of success.

CONCLUSIONS

Axial-load fatigue-crack-growth tests were conducted on 12-inch wide, 0.090-inch thick specimens made of 7075-T6 and 2024-T3 aluminum alloys. These tests were performed to study fatigue-crack-growth behavior at high stress levels, and to determine the ability of the elastic stress-intensity analysis, and of a separate modified stress-intensity analysis derived by combining Rice's cyclic stress-intensity method with the modified (for plasticity) stress-intensity methods developed by Irwin, Dugdale, and Newman to correlate the data generated in this investigation and in the investigation reported in NASA TN D-5390. The stress levels applied in this investigation ranged from 55 to 72.5 ksi for the 7075-T6 and from 30 to 52.5 ksi for the 2024-T3. The stress ratios (ratio of the minimum stress to the maximum stress) ranged from 0 to 0.7. The following conclusions were drawn from this investigation.

1. For a given R value, fatigue-crack-growth rates in 7075-T6 were nominally a single-valued function of the elastic stress-intensity range and of the modified stress-intensity ranges.

2. For a given R value, fatigue-crack-growth rates in

2024-T3 below a value of 1×10^{-4} in./cycle were nominally a single-valued function of the elastic stress-intensity range and of the modified stress-intensity ranges. However, crack growth rates in the 2024-T3 above approximately 1×10^{-4} in./cycle exhibit an ordering according to values of the maximum applied stress for all methods.

3. The fatigue-crack-growth in 7075-T6 appear to become unstable and static fracture occurred as the fatigue-crack-growth rates approached 4×10^{-2} in./cycle. However, stable fatigue-crack-growth rates up to 4×10^{-1} in./cycle were observed in 2024-T3.

4. A reflex curvature occurred in plots of crack growth rate against stress-intensity range at the higher R values for both 7075-T6 and 2024-T3.

REFERENCES

1. Castle, Claude B.; and Ward, John F.: Fatigue Investigation of Full-Scale Wing Panels of 7075 Aluminum Alloy. NASA TN D-635, 1961.

2. Hudson, C. Michael: Effect of Stress Ratio on Fatigue-Crack Growth In 7075-T6 and 2024-T3 Aluminum-Alloy Specimens. NASA TN D-5390, 1969.

3. Rice, J. R.: Mechanics of Crack Tip Deformation and Extension by Fatigue. Fatigue Crack Propagation. ASTM STP 415, June 1967.

4. Irwin, G. R.: Plastic Zone Near a Crack and Fracture Toughness. Proceedings of the Seventh Sagamore Ordnance Materials Research Conference. Syracuse University Research Institute, August, 1960.

5. Dugdale, D. S.: Yielding of Steel Sheets Containing Slits, Journal of Mechanics and Physics of Solids, Vol. 8, 1960.

6. Newman, J. C., Jr.: Fracture of Cracked Plates Under Plane Stress. Int. J. of Eng. Fracture Mech., Vol. 1, No. 1, 1968.

7. Grover, H. J.; Bishop, S. M.; and Jackson, L. R.: Fatigue Strengths of Aircraft Materials. Axial-Load Fatigue Tests on Unnotched Sheet Specimens of 24S-T3 and 75S-T6 Aluminum Alloys and of SAE 4130 Steel. NACA TN 2324, 1951.

8. Hudson, C. Michael; and Hardrath, Herbert F.: Investigation of the Effects of Variable-Amplitude Loadings on Fatigue Crack Propagation Patterns. NASA TN D-1803, 1963.

9. Paris, Paul C.: The Fracture Mechanics Approach to Fatigue. Fatigue--An Interdisciplinary Approach, John J. Burke, Norman L. Reed, and Volker Weiss, eds., Syracuse University Press, 1964, pp. 107-132.

10. Broek, D.; and Schijve, J.: The Influence of the Mean Stress on the Propagation of Fatigue Cracks in Aluminum Alloy Sheet. NLR-TR M. 2111, 1963.

APPENDIX

METHODS OF ANALYSIS

Linear Elastic Stress Intensity Analysis

The linear elastic stress intensity factor is a local stress parameter which reflects the intensity of the elastic stresses at all points surrounding the tip of a crack. For engineering materials however, some plastic deformation always occurs at the crack tip during the application of a stress. The greater this plastic deformation, the less accurately the elastic stress intensity factor reflects the stress conditions around the crack tip. Fortunately, the plastic deformations usually associated with the growth of fatigue cracks are relatively small, and the stress intensity factor can be used successfully to correlate fatigue crack growth data, see references 2, 9, and 10. Because of this previous successful correlation, the elastic stress intensity analysis was used as a starting point for analyzing the fatigue-crack-growth data generated in this investigation.

The basic relationship between rate of fatigue-crack-growth and the stress intensity factor was first proposed by Paris, ref. 9, and is given by

$$da/dN = f(\Delta K) \tag{1A}$$

where

$$\Delta K = K_{max} - K_{min} \tag{2A}$$

For centrally-cracked sheet specimens subjected to a uniformly distributed axial load

$$K_{max} = \alpha S_{max} (\pi a)^{1/2} \tag{3A}$$

and

$$K_{min} = \alpha S_{min} (\pi a)^{1/2} \tag{4A}$$

The term α is a factor which corrects for the finite width of the specimen and is given by

$$\alpha = \left(\sec \frac{\pi a}{w}\right)^{1/2} \tag{5A}$$

Modified Stress Intensity Analysis

A rationale for calculating a modified sress-intensity factor for cyclic loading conditions was developed by Rice, ref. 3. Basic to the development of this rationale are the assumptions that (1) the crack does not close throughout the loading cycle, and (2) that all plastic deformations involve proportional flow, i.e., components of the plastic strain tensor remain in constant proportion to one another at each point of the plastic region.

During the loading portion of the fatigue cycle, a plastic zone forms at the tip of a fatigue crack. An analytical solution for the stresses in the vicinity of this plastic zone is presented in reference 3. Rice proposed that when the fatigue loading is reduced to the minimum load, reversed plastic deformations occur at the crack tip forming a new plastic zone and that the stresses in the vicinity of this new plastic zone are given by a solution identical to that for the initial loading, but with the loading parameter replaced by the loading reduction, and the yield stress replaced by twice its

value for the original loading. Rice superposed the stress solution for the loading portion of the cycle (at maximum load) with the solution for the unloading portion of the cycle (to minimum load) to obtain the magnitude and sign of the stresses near the crack tip when the minimum load is reached. For subsequent loading cycles, Rice showed that the cyclic variation in the stresses near the crack tip depended only on the loading variation (from maximum load to minimum load), and were independent of the maximum loading. Consequently, the range of the stress intensity factor (which reflects the intensity of these stresses) depends only on the variation in applied stress and is given by:

$$\Delta K = \alpha \quad \Delta S \left(\quad \pi a \right)^{1/2} \tag{6A}$$

Irwin, ref. 4; Dugdale, ref. 5; and Newman, ref. 6; developed a plasticity correction for the linear elastic stress-intensity factor. These three investigators developed the same basic modification to the elastic stress-intensity factor, i.e., the length of the plastic zone ahead of the crack tip ρ was added to the half crack length a to calculate a modified stress intensity factor. A large quantity of fracture toughness data on relatively tough material has been correlated with varying degrees of success by using the modified stress intensity factors, ref. 6.

The only difference between Irwin's, Dugdale's, and Newman's modification is the equation used to calculate the length of the plastic zone. Their equations for the length of the plastic zone in finite width sheets are listed as follows:

Irwin $$\rho_{(Irwin)} = \frac{1}{2\pi}\left(\frac{\alpha S\sqrt{\pi a}}{\sigma_y}\right)^2 \quad (7A)$$

Dugdale $$\rho_{(D)} = a\left[\frac{w}{\pi a}\arcsin\left(\sin\frac{\pi a}{w}\sec\frac{\pi S}{2\sigma_y}\right) - 1\right] \quad (8A)$$

Newman $$\rho_{(N)} = A\,a\left[\frac{w}{\pi a}\arcsin\left(\sin\frac{\pi a}{w}\sec\frac{\pi S}{2B\sigma_y}\right) - 1\right] \quad (9A)$$

Values of the material constants A and B used to calculate the plastic zone size, as proposed by Newman (ref. 6), are given in the following table:

Material	A	B
7075-T6	0.693	1.025
2024-T3	0.699	1.098

In the investigation reported herein the concepts of cyclic stress intensity developed by Rice, and the plasticity correction proposed by Irwin, Dugdale, and Newman were combined to calculate modified stress intensity factors. That is, equation (6A) was used to calculate a modified stress-intensity range. In making these calculations, however, the length of the plastic zone at the crack tip, ρ, was added to the half-crack length a, in equation (6A). In calculating these plastic zone lengths (equations 7A, 8A, and 9A), $2\sigma_y$ was substituted for σ_y, and the change in stress was substituted for the applied stress as proposed by Rice, ref. 3. The ability of the three modified stress intensity ranges (i.e., modified using equations 7A, 8A, and 9A) to correlate the data was studied.

Table 1. - AVERAGE TENSILE PROPERTIES OF MATERIALS TESTED

(1968 DATA)

Material	Ultimate tensile strength ksi	Yield stress (0.2-percent offset) ksi	Young's modulus of elasticity ksi	Elongation in 2-inch gage length, percent	No. of tests
7075-T6	83.2	75.5	10 100	12	20
2024-T3	70.9	51.2	10 420	31	20

TABLE 2. FATIGUE CRACK GROWTH DATA FOR 7075-T6 ALUMINUM ALLOY

R = 0

S_{max} = 55 ksi		S_{max} = 60 ksi		S_{max} = 65 ksi		S_{max} = 70 ksi		S_{max} = 72.5 ksi	
Cycles	a in.	Cycles	a in.	Cycles	a in.	Cycles	a in.	Cycles	a in.
533	.082	313	.080	218	.084	148	.089	91	.084
577	.085	347	.085	224	.090	158	.098	93	.089
620	.089	378	.106	234	.100	166	.112	96	.093
664	.097	403	.118	246	.105	168	.116	98	.095
699	.105	426	.133	249	.109	171	.125	100	.099
727	.117	448	.150	254	.115	173	.133	101	.102
750	.130	458	.163	262	.128	175	.140	102	.105
768	.138	463	.170	269	.133	176	.146	103	.110
782	.150	470	.178	276	.148	178	.150	104	.117
792	.155	479	.195	281	.158				
803	.172	482	.203	283	.168				
820	.182	485	.208	285	.178				
830	.200	487	.213	286	.184				
841	.218	489	.218	287	.186				
849	.224	490	.223	288	.193				
855	.240								
861	.252								
864	.265								
866	.268								
869	.345								

R = 0.33

S_{max} = 60 ksi		S_{max} = 65 ksi		S_{max} = 70 ksi		S_{max} = 72.5 ksi	
Cycles	a in.	Cycles	a in.	Cycles	a in.	Cycles	a in.
708	.080	499	.087	350	.089	273	.080
790	.089	515	.096	370	.092	279	.081
828	.095	530	.103	380	.102	283	.082
888	.112	551	.119	390	.114	285	.085
915	.125	570	.131	395	.122	287	.087
925	.134	590	.155	396	.123		
939	.141	595	.160	398	.125		
951	.148	599	.164	399	.126		
975	.163	605	.171				
990	.175	609	.176				
1001	.186	613	.194				
1005	.193						
1010	.201						
1022	.224						
1026	.240						
1032	.248						
1037	.255						

TABLE 2. (CONCLUDED) FATIGUE CRACK GROWTH DATA FOR 7075-T6 ALUMINUM ALLOY

R = 0.5

S_{max} = 60 ksi		S_{max} = 65 ksi		S_{max} = 70 ksi		S_{max} = 72.5 ksi	
Cycles	a in.	Cycles	a in.	Cycles	a in.	Cycles	a in.
1427	.084	1099	.083	597	.080	550	.080
1525	.095	1133	.093	640	.090	604	.089
1565	.100	1167	.100	662	.100	607	.093
1598	.110	1201	.113	690	.112	614	.097
1701	.120	1225	.125	695	.120	620	.111
1733	.133	1245	.140	701	.125	623	.114
1767	.140	1258	.165	705	.129	627	.118
1799	.155	1263	.170	710	.133	630	.126
1833	.170	1268	.183	713	.135	632	.134
1868	.185	1275	.195	715	.136		
1900	.220						
1907	.230						
1911	.240						
1913	.250						

R = 0.7

S_{max} = 60 ksi		S_{max} = 65 ksi		S_{max} = 70 ksi	
Cycles	a in.	Cycles	a in.	Cycles	a in.
4850	0.113	2695	.084	2638	.083
5143	.134	3062	.095	2864	.095
5338	.152	3341	.113	2966	.114
5434	.170	3525	.134	3054	.135
5506	.183	3557	.148	3128	.157
5604	.213	3571	.155	3148	.165
5700	.240	3599	.165	3152	.170
5727	.260	3647	.188	3160	.175
5751	.265	3664	.196	3164	.179
5766	.275	3674	.204	3167	.185
5788	.285	3680	.210		
5818	.303	3687	.214		
5826	.310				
5850	.334				

TABLE 3. FATIGUE CRACK GROWTH DATA FOR 2024-T3 ALUMINUM ALLOY

R = 0

S_{max} = 30 ksi		S_{max} = 40 ksi		S_{max} = 50 ksi		S_{max} = 52.5 ksi	
Cycles	a in.	Cycles	a in.	Cycles	a in.	Cycles	a in.
114	.500	1344	.090	443	.130	151	.085
267	.600	1587	.120	467	.150	161	.095
369	.700	1830	.196	508	.200	178	.100
434	.800	2010	.260	523	.250	191	.110
484	.900	2120	.360	528	.300	200	.118
524	1.000	2151	.420	529	.350	205	.130
554	1.100	2193	.560	530	.400	213	.140
579	1.200	2202	.610	530	.450	218	.148
598	1.300	2213	.700			222	.155
613	1.400	2220	.770			225	.165
625	1.500	2223	.820			228	.175
634	1.600	2229	.930			230	.230
641	1.700	2233	1.020				
647	1.800	2235	1.090				
652	1.900	2237	1.140				
656	2.000	2238	1.210				
660	2.100	2239	1.240				
663	2.200	2240	1.290				
665	2.300	2241	1.370				
667	2.400	2242	1.420				
668	2.500	2243	1.580				
669	2.600						
670	2.700						
671	2.800						
672	2.900						

R = 0.33

S_{max} = 30 ksi		S_{max} = 40 ksi		S_{max} = 50 ksi		S_{max} = 52.5 ksi	
Cycles	a in.	Cycles	a in.	Cycles	a in.	Cycles	a in.
377	.900	169	.240	79	.148	513	.085
477	1.000	373	.290	91	.170	534	.095
577	1.100	546	.330	142	.200	575	.110
622	1.200	751	.430	184	.225	597	.115
676	1.300	955	.620	216	.270	639	.132
719	1.400	1005	.720	219	.275	653	.145
751	1.500	1049	.830	221	.280	665	.148
779	1.600	1063	.890	227	.296	671	.150
801	1.700	1078	.970	229	.305	674	.155
819	1.800	1093	1.070	231	.315	678	.162
833	1.900	1105	1.160	232	.328	682	.180
843	2.000	1108	1.200	233	.342		
852	2.100	1113	1.250	234	.440		
859	2.200	1117	1.310				
864	2.300	1119	1.350				
868	2.400	1122	1.410				
871	2.500	1124	1.450				
873	2.600	1125	1.480				
874	2.700	1126	1.520				
875	2.800	1127	1.570				
876	2.900	1128	1.650				
877	3.000	1129	1.800				

TABLE 3. (CONCLUDED) FATIGUE CRACK GROWTH DATA FOR 2024-T3 ALUMINUM ALLOY

R = 0.5

S_{max} = 30 ksi		S_{max} = 40 ksi		S_{max} = 50 ksi		S_{max} = 52.5 ksi	
Cycles	a in.	Cycles	a in.	Cycles	a in.	Cycles	a in.
107	1.200	117	.440	227	.180	954	.092
202	1.250	281	.490	272	.188	995	.105
278	1.300	363	.510	315	.200	1080	.115
398	1.400	445	.530	379	.218	1143	.122
504	1.500	527	.560	400	.228	1185	.140
594	1.600	609	.610	432	.242	1215	.155
665	1.700	691	.650	448	.255	1219	.165
717	1.800	736	.680	450	.258	1229	.170
762	1.900	798	.730	456	.262	1233	.182
802	2.000	840	.770	460	.265	1234	.208
836	2.100	882	.820	466	.268		
866	2.200	924	.870	470	.272		
888	2.300	945	.910	474	.285		
904	2.400	987	.980	478	.292		
917	2.500	1006	1.020	482	.298		
927	2.600	1016	1.040	486	.310		
634	2.700	1026	1.080	488	.315		
939	2.800	1036	1.110	489	.318		
941	2.900	1043	1.130	490	.338		
942	3.000	1047	1.150	491	.355		
943	3.050	1051	1.170	492	.498		
		1056	1.210				
		1061	1.220				
		1065	1.250				
		1069	1.270				
		1071	1.280				
		1073	1.300				
		1075	1.310				
		1077	1.340				
		1078	1.350				
		1079	1.390				
		1080	1.430				
		1081	1.640				

R = 0.7

S_{max} = 30 ksi		S_{max} = 40 ksi		S_{max} = 50 ksi		S_{max} = 52.5 ksi	
Cycles	a in.	Cycles	a in.	Cycles	a in.	Cycles	a in.
655	1.000	95	.760	300	.230	1400	.082
872	1.080	330	.820	420	.245	2163	.110
1089	1.090	672	.920	595	.260	2339	.120
1337	1.100	798	1.000	701	.275	2479	.125
1603	1.160	1001	1.110	726	.280	2620	.135
2011	1.220	1050	1.150	750	.285	2722	.140
2568	1.330	1105	1.210	824	.290	2773	.150
3115	1.430	1160	1.260	873	.295	2794	.155
3672	1.590	1200	1.330	928	.305	2815	.165
4032	1.690	1212	1.340	983	.315		
4411	1.870	1216	1.360	1015	.325		
4698	2.010	1225	1.370	1060	.335		
4906	2.170	1236	1.380	1104	.345		
5015	2.290	1240	1.390	1126	.350		
5058	2.350	1251	1.430	1137	.360		
5069	2.386	1259	1.450	1148	.365		
5102	2.430	1263	1.460	1153	.380		
5124	2.480	1267	1.500	1154	.385		
5129	2.510	1269	1.530	1155	.390		
5134	2.520	1271	1.550	1156	.410		
5139	2.530	1273	1.660	1157	.470		
5144	2.550						
5144	2.620						
5158	3.120						

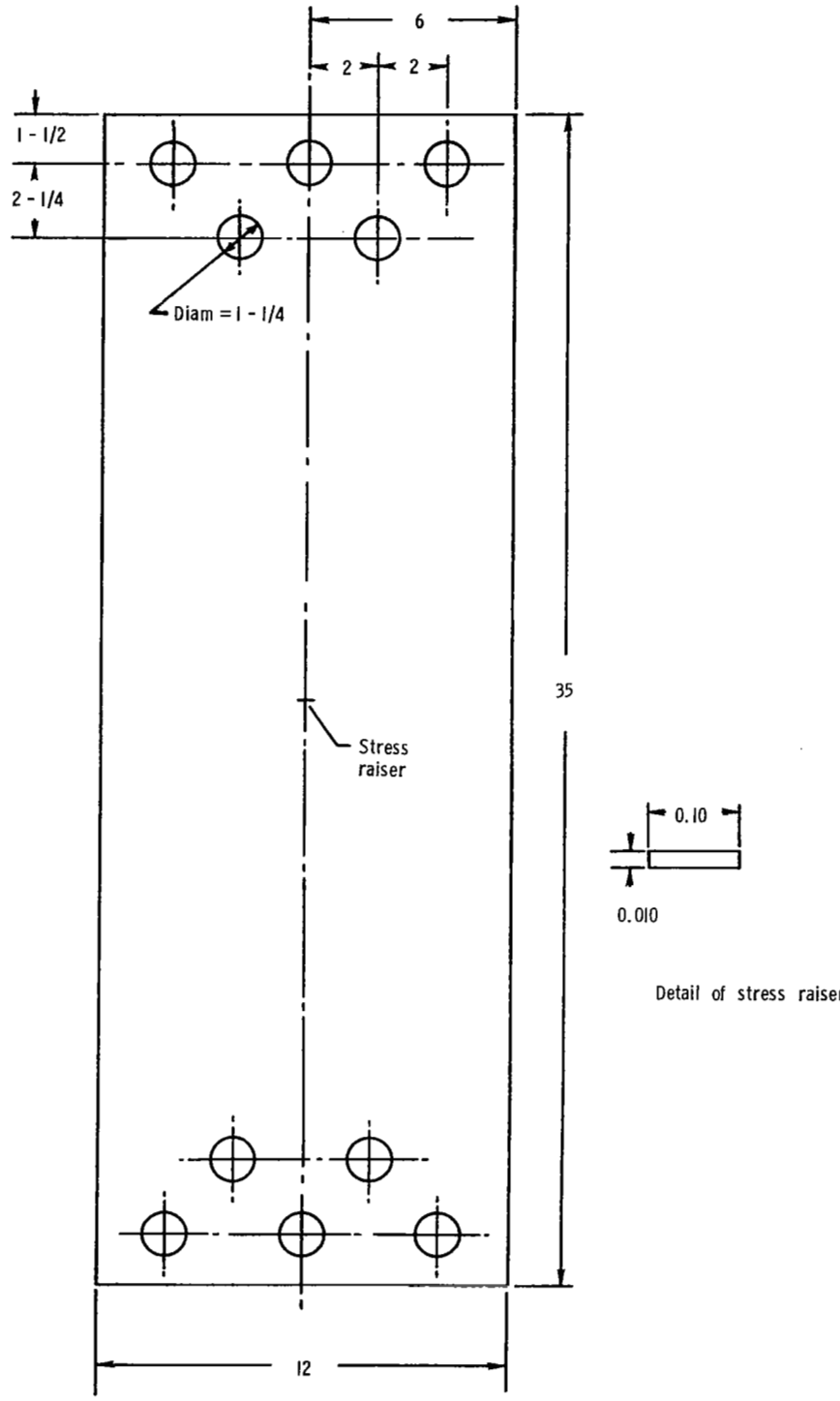

Figure 1. Specimen Configuration (all dimensions in inches)

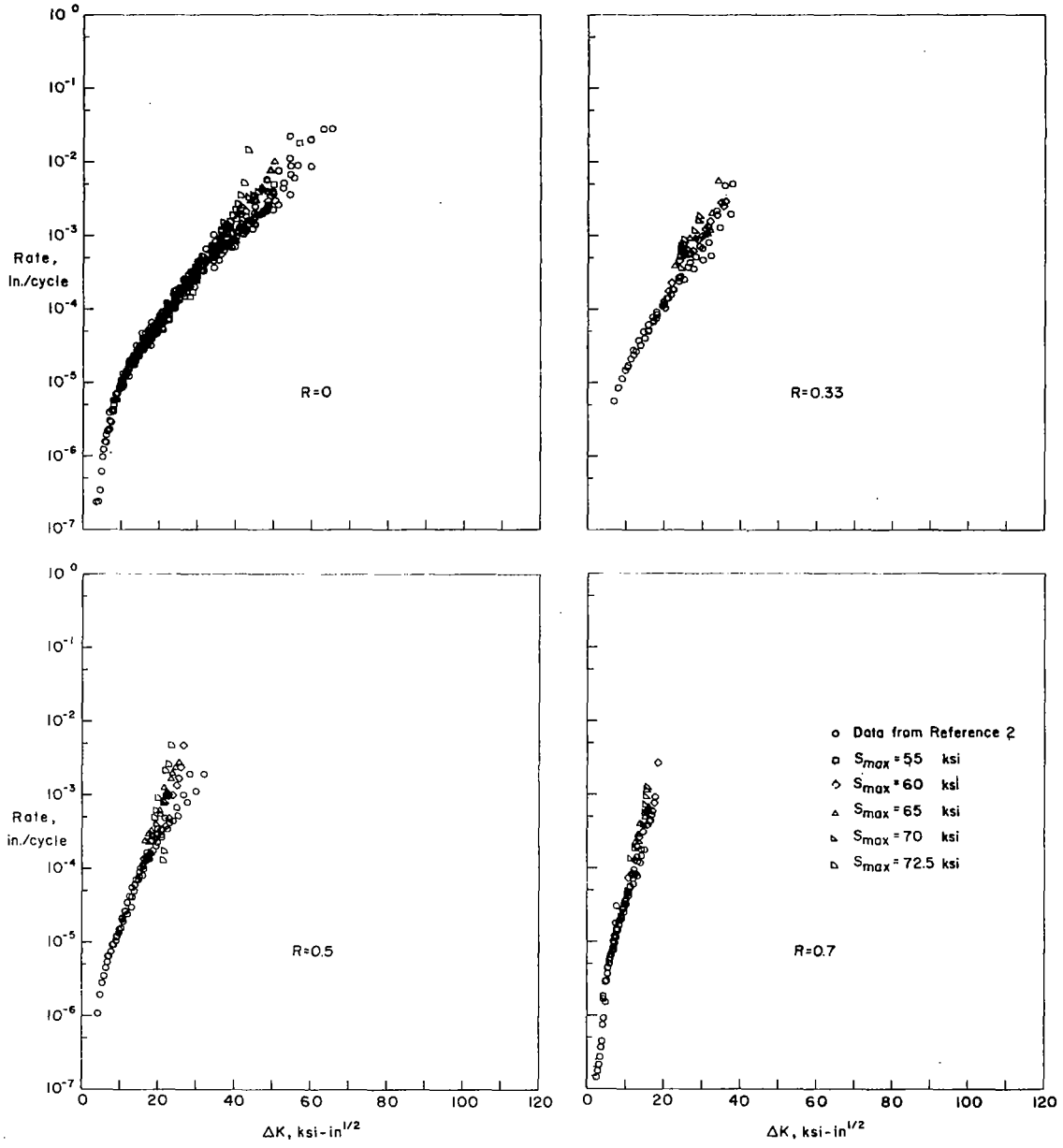

(a) 7075-T6 alloy

Figure 2. Relationship between fatigue-crack-growth and the elastic stress-intensity range.

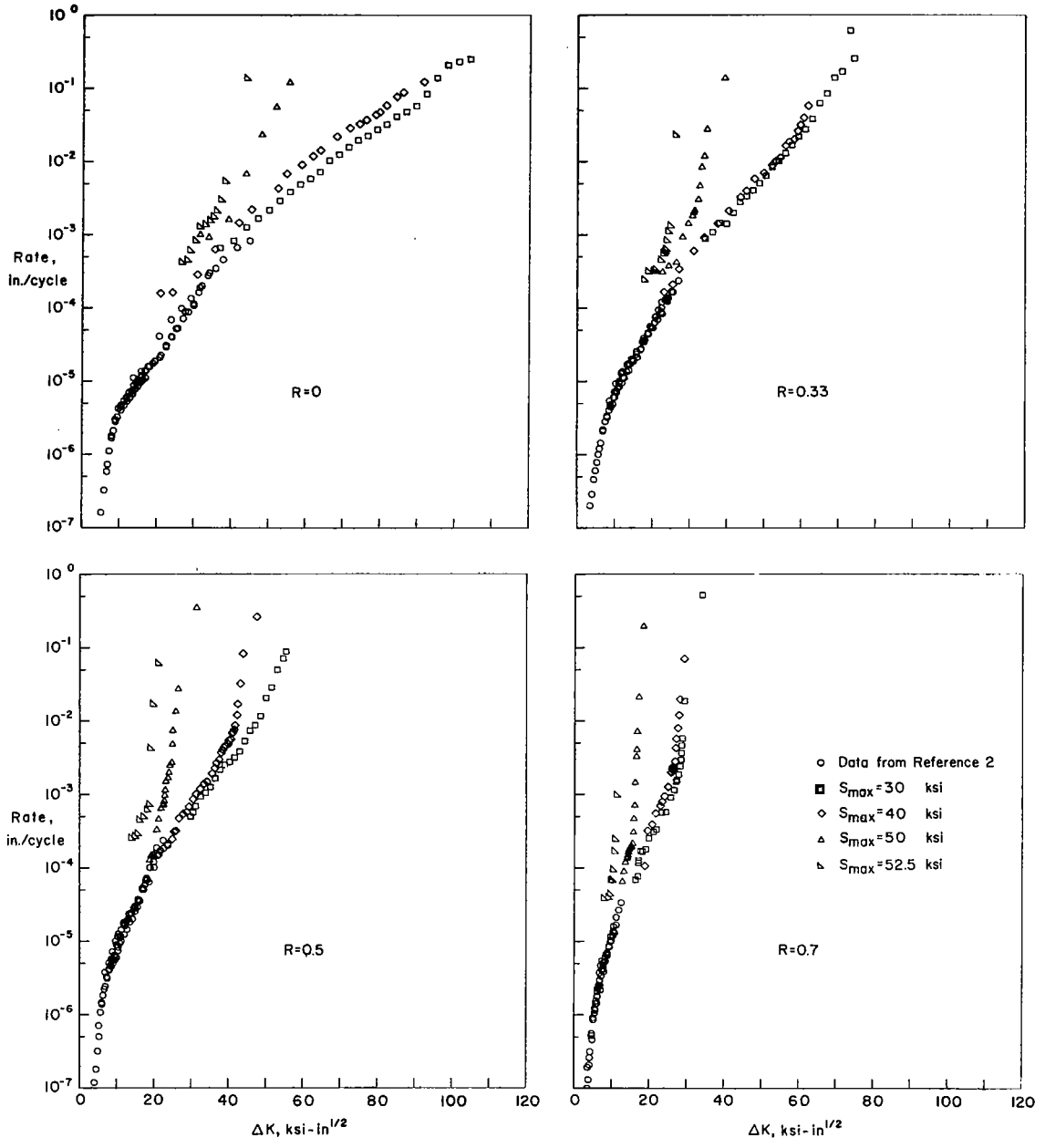

(b) 2024-T3 alloy

Figure 2. Concluded.

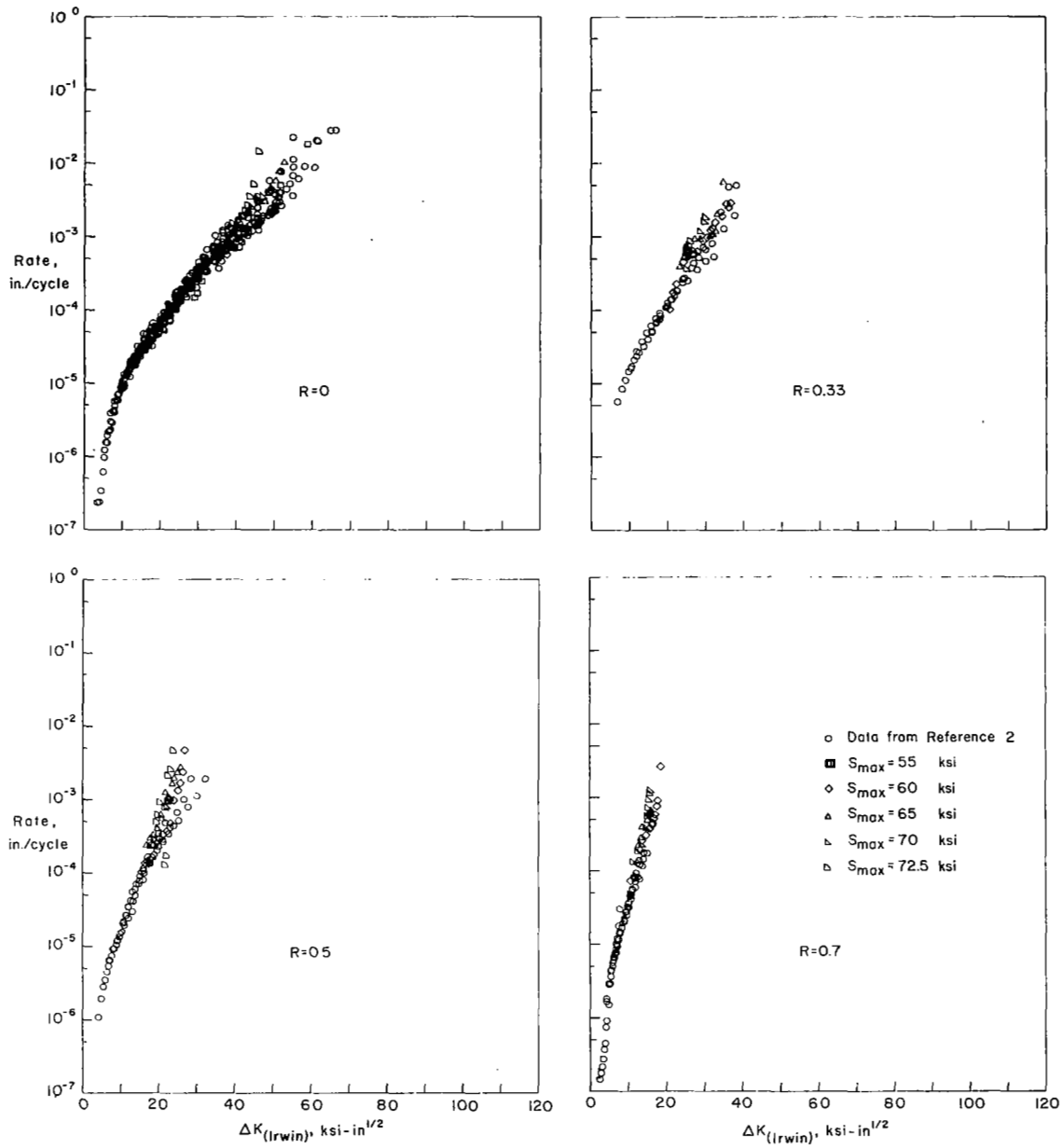

(a) Irwin's Plasticity Correction

Figure 3. Relationship between fatigue-crack-growth and the modified cyclic stress-intensity ranges including the plasticity corrections for the 7075-T6 alloy.

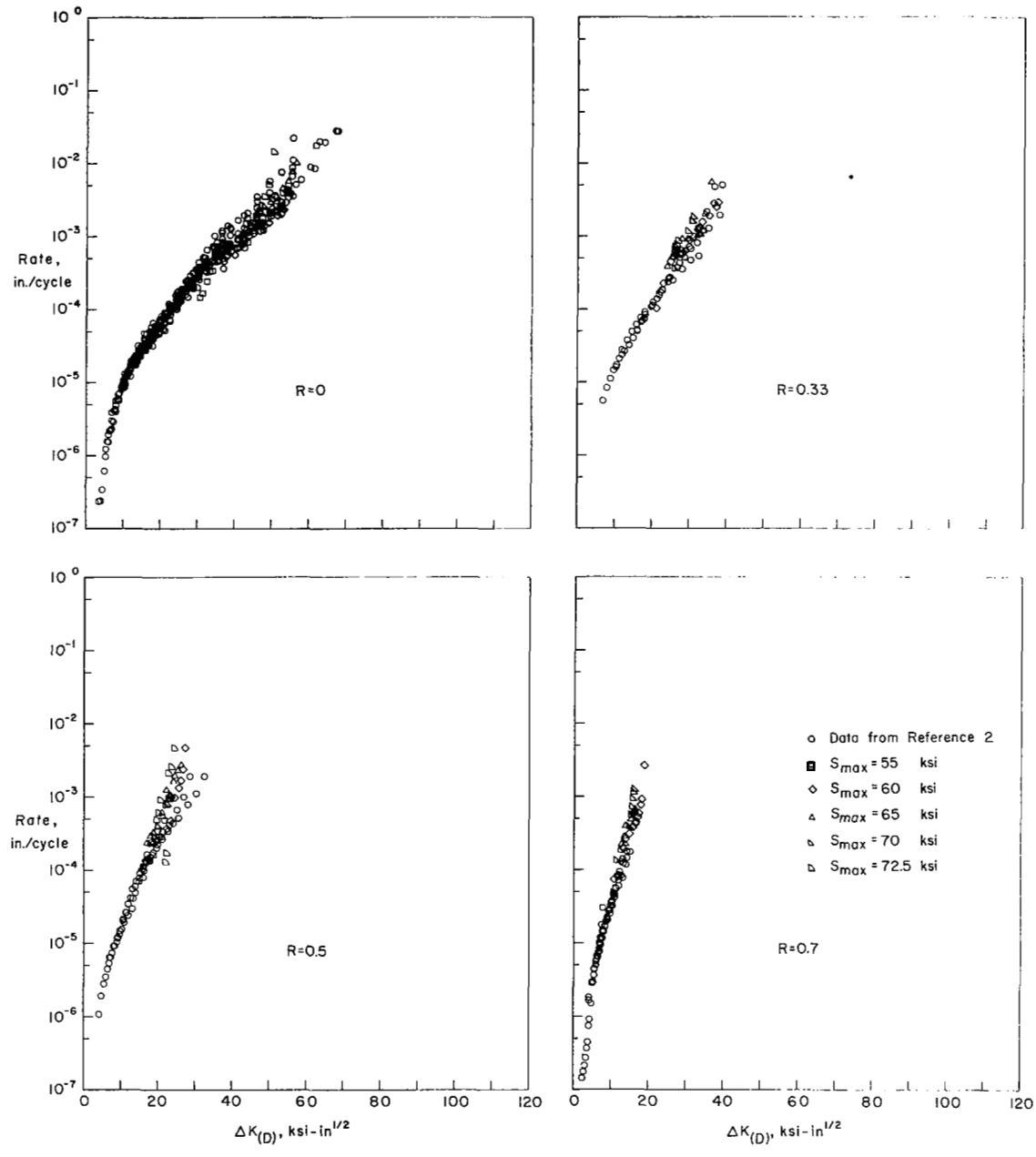

(b) Dugdale's Plasticity Correction

Figure 3. Continued.

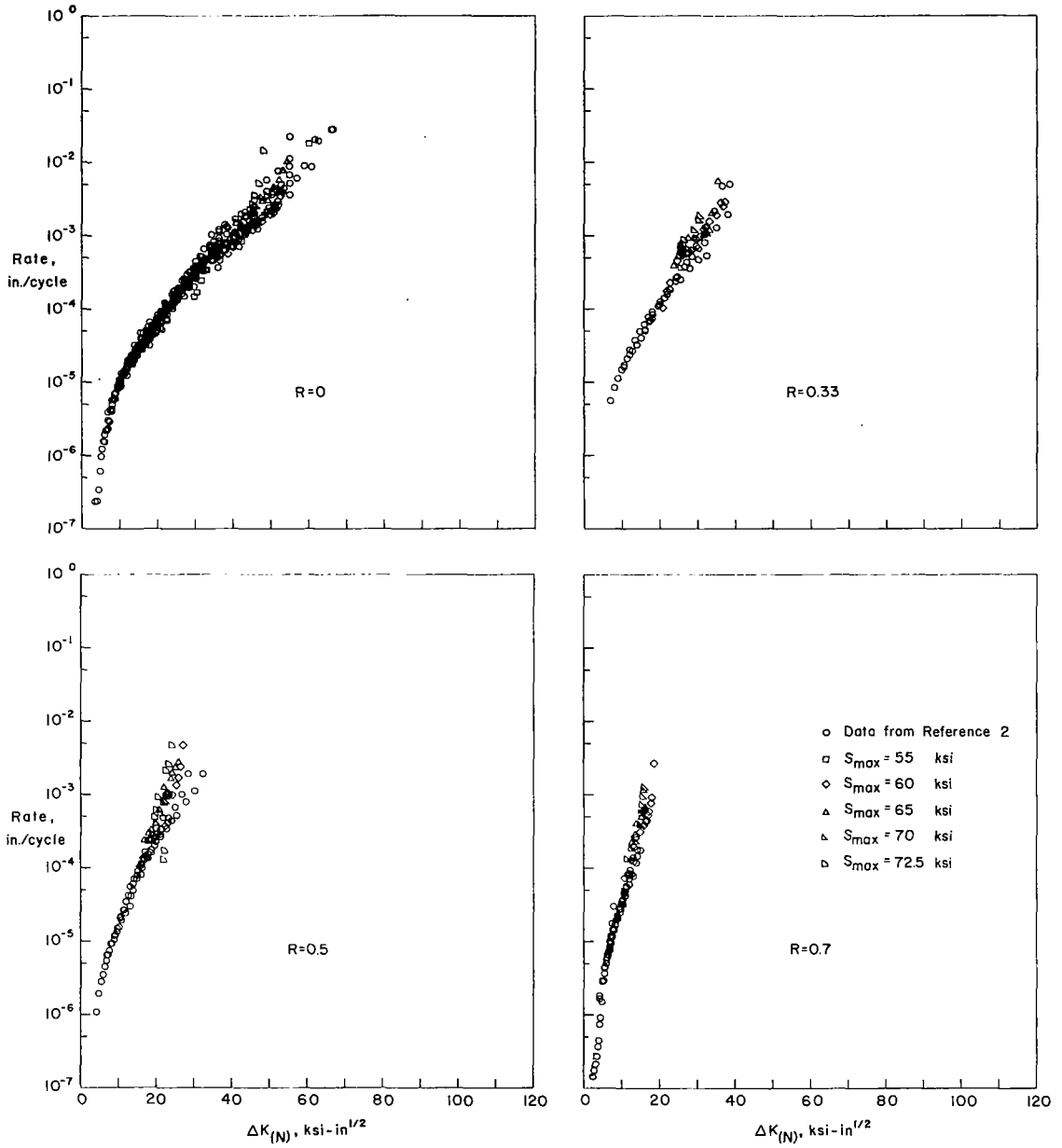

(c) Newman's Plasticity Correction

Figure 3. Concluded.

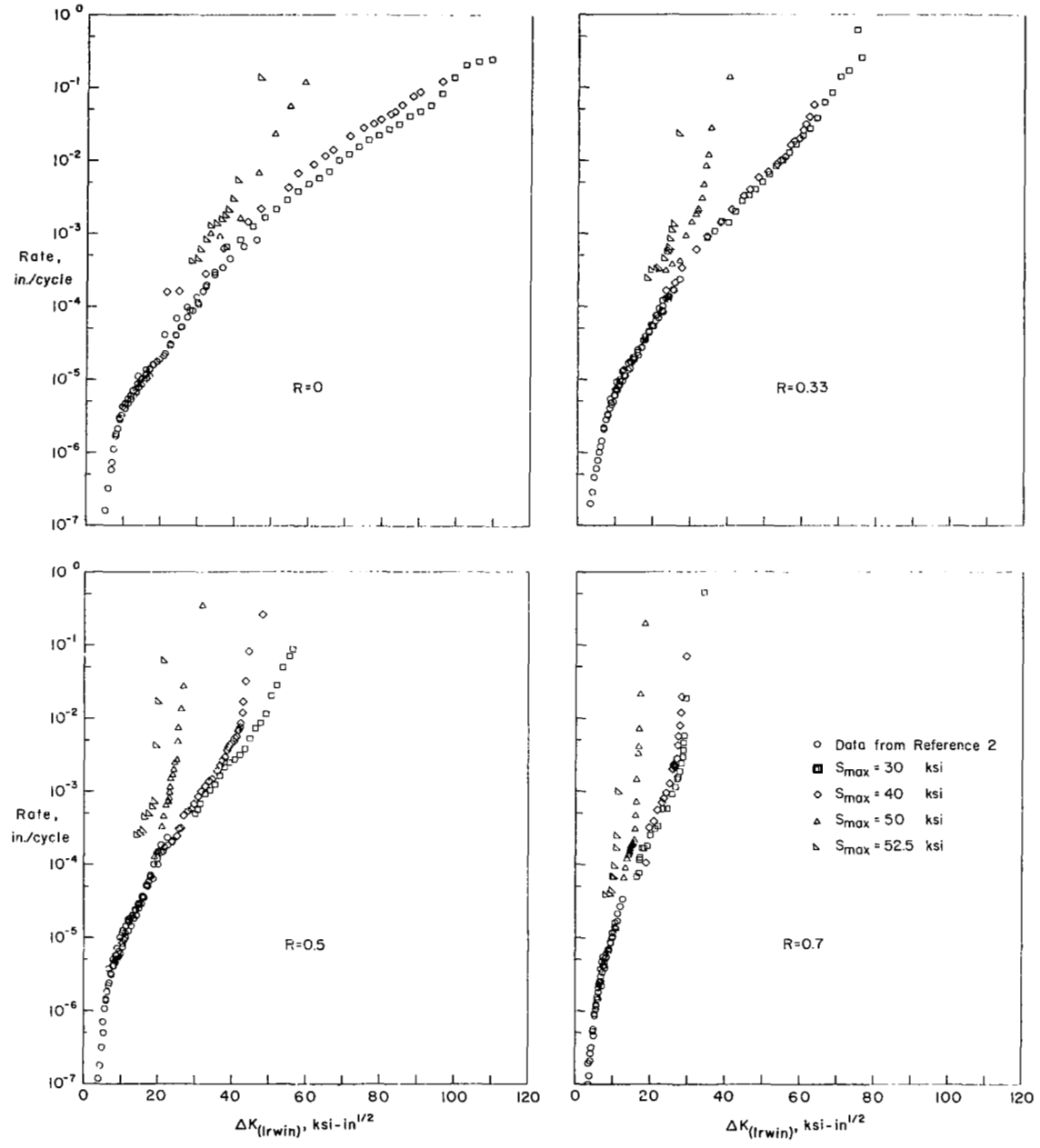

(a) Irwin's Plasticity Correction

Figure 4. Relationship between fatigue-crack-growth and the modified cyclic stress-intensity ranges including the plasticity corrections for the 2024-T3 alloy.

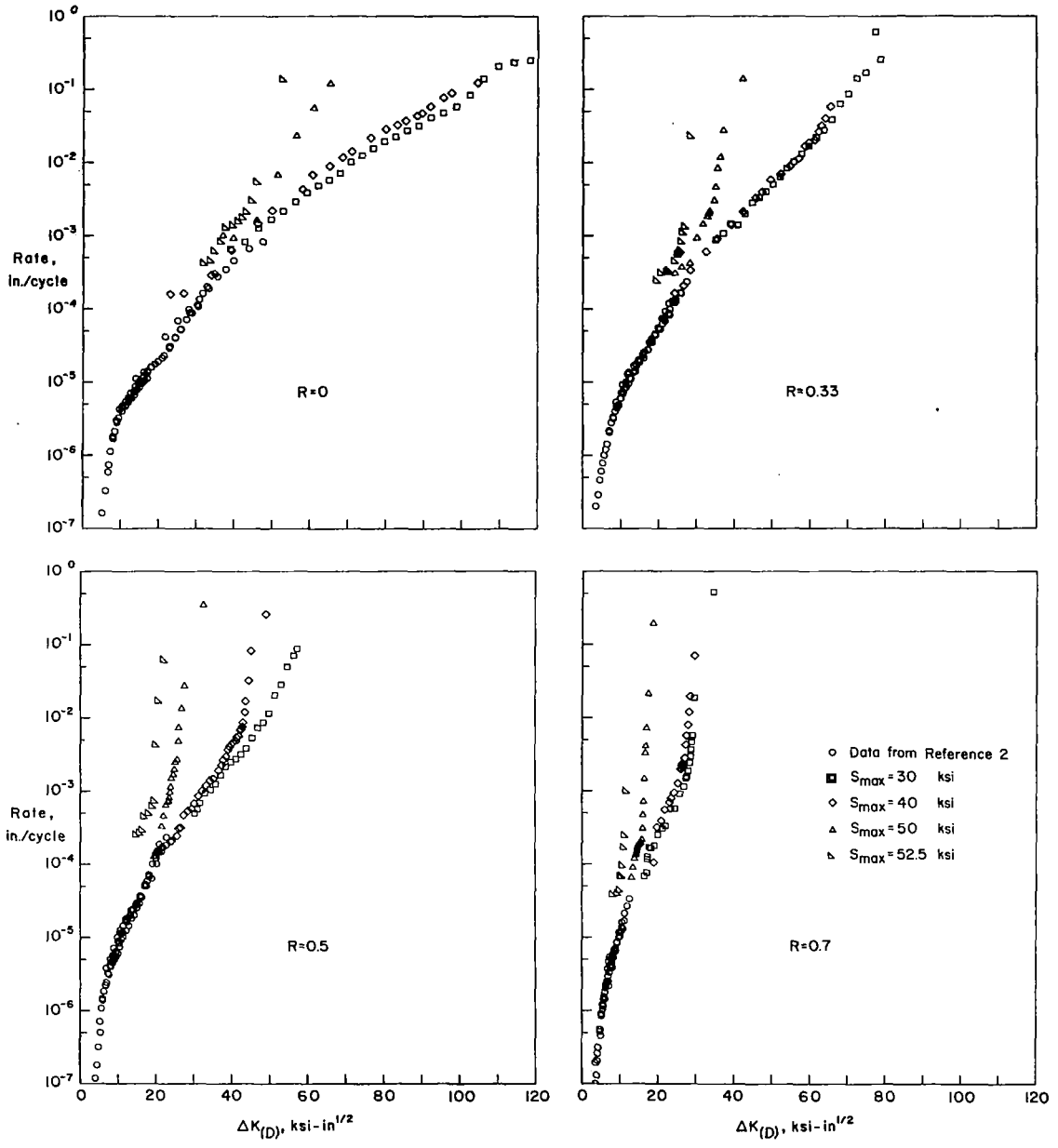

(b) Dugdale's Plasticity Correction

Figure 4. Continued.

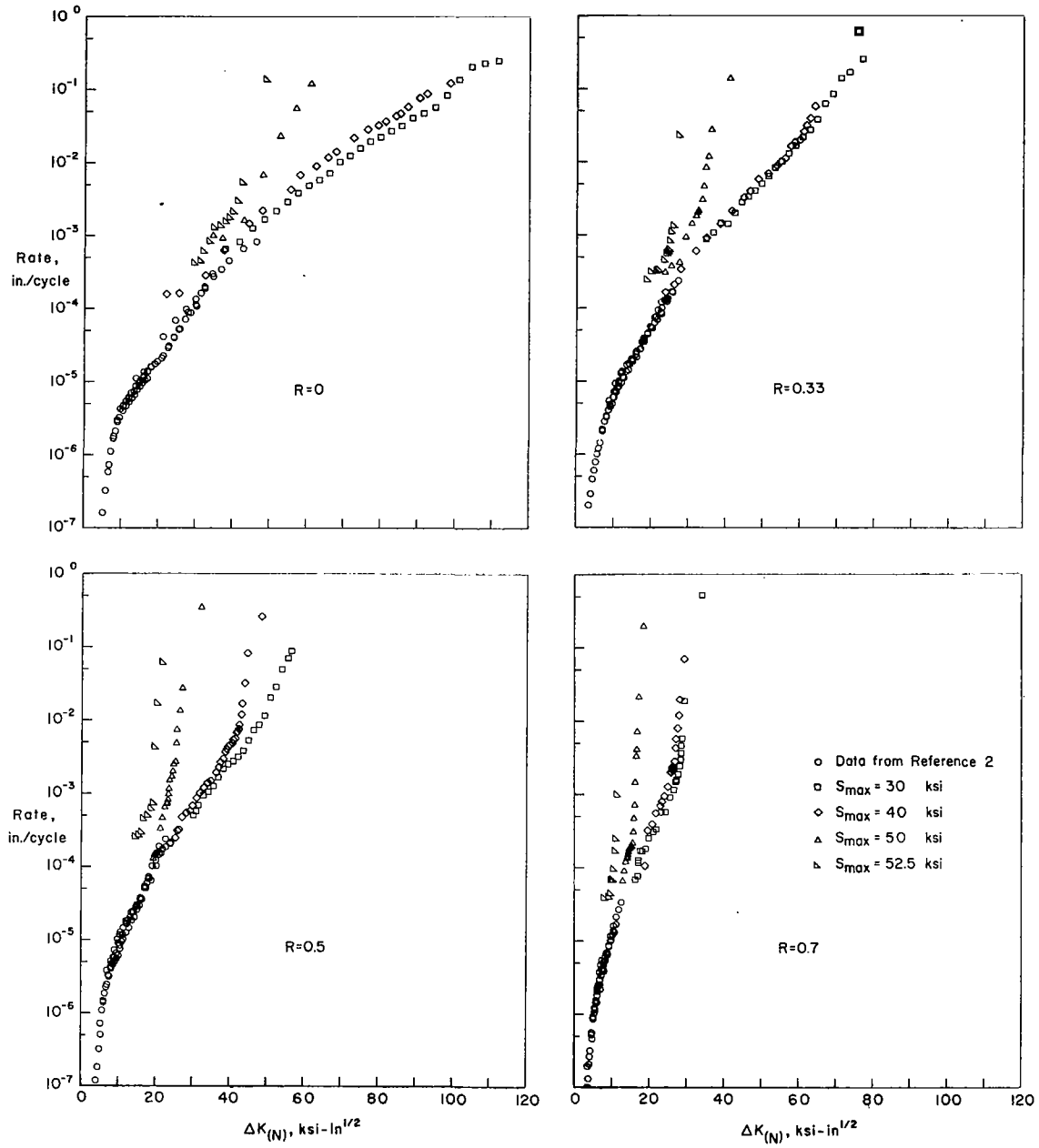

(c) Newman's Plasticity Correction

Figure 4. Concluded.